Commensurability of QPO Frequencies in BHXRB

Prerna Rana[1,†] A. Mangalam[1,‡]
[1] Indian Institute of Astrophysics, Sarjapur Road, Koramangala, Bangalore, 560034, India
prernarana@iiap.res.in[†], mangalam@iiap.res.in[‡]

May 15, 2018

Abstract

We study equatorial eccentric orbits in Kerr geometry and apply relativistic precession model to the cases of black hole X-ray binaries (BHXRB) where two HFQPOs (High-Frequency Quasi-Periodic Oscillations) and Type-C QPO are simultaneously observed, or to the cases where only two simultaneous HFQPOs are observed, for example in GROJ1655-40, M82X-1, XTEJ1550-564, 4U1630-47, and GRS1915+105. We assume that the frequencies to be Gaussian or Gamma distributed and calculate probability distributions to infer eccentricity e, periastron distance r_p, of the orbit giving rise to QPOs, and the spin of the black hole, a. In the equatorial case, we find that the eccentric solutions are found in the region between ISCO and the marginally bound orbit. We also establish the primacy of eccentric orbits in this region for the generation of 3:2 ($\mathcal{R} = \nu_\phi/(\nu_\phi - \nu_r) \simeq 1.5$) commensurability of QPOs as a strong possibility. We also explore the dynamical parameter space to produce commonly found fundamental frequency ratios for spherical ($Q \neq 0$) bound trajectories in the coronal region.

1 Introduction

BHXRB are the systems with a primary black hole and a non-degenerate secondary star. QPOs with frequencies higher than 40 Hz, called HFQPOs, are key to study the regions very near to the black hole. There are also the cases of BHXRB which have shown two simultaneous high-frequency QPOs where their specific frequency ratios are approximately commensurate: 3:2, 5:3, 2:1, 3:1 and 4:1, [4]. Whereas, GROJ1655-40, M81 X-1 are known to show the detection of three simultaneous QPOs [11, 14].

We first take up the specific application of relativistic precession to HFQPOs that come in pairs and study the possible regions around black hole giving rise to 3:2 commensurability. We study equatorial eccentric to investigate the HFQPO commensurability regions around Kerr black hole. We also show that the region inside innermost stable circular orbit (ISCO) is a probable site for the generation of QPOs with 3:2 ratio. Next, we take up in detail, the cases of BHXRBs where three or two simultaneous HFQPOs have been detected. We attribute them to the RP model and calculate the parameters $\{e, \mu, a\}$ of the equatorial eccentric orbits which are possibly giving rise to these QPOs, using frequency formulae derived in [15]. We see that eccentric orbits inside ISCO radius are highly probable candidates for 3:2 commensurability.

2 Relativistic precession and QPOs in BHXRB

We study equatorial eccentric to investigate the possible regions of generation of QPO commensurability around a Kerr black hole. Assuming the RP model for QPOs, we study the region of origin of these QPOs in the (e, r_p) plane for different values of a and also in the (a, r_p) plane for different values of e, Fig. 1. We see from Figs. 1(a) & 1(b) that in (a, r_p) plane as the eccentricity increases, the 3:2, 5:3 and 2:1 ratio contours move inside ISCO, which explains that these simultaneous QPO signals could be originating from eccentric orbits in the region between ISCO and circular innermost marginally bound orbit (CIMBO), which we call as orifice region. Also, we see from Figs. 1(c) & 1(d) that in (e, r_p) plane as the spin parameter increases, the ratio contours move slightly outward, where the high eccentric orbits are in the orifice region.

Next, we take all the possible allowed combinations of parameters (e, r_p, a) for the eccentric orbits and calculate $\mathcal{R} = \nu_\phi/(\nu_\phi - \nu_r)$ using the frequency formulae derived in [15] and split the parameter volume into three sets. The first set corresponds to all the orbits that lie in the orifice; we call this as the orifice set. The second set corresponds to all the allowed orbits that lie in between ISCO and $10r_g$, we call it as the disk set, and the third set, called the union set, is the union of the first two. Fig. 2(d) shows the probability density distribution, $P(\mathcal{R})$, for these three regions and it peaks between $\mathcal{R}$ =1.5-1.7 only for the orifice set, whereas for the disk and union sets $P(\mathcal{R})$ peaks between $\mathcal{R}$ =2-3. This makes the argument for the origin of 3:2 commensurability from the eccentric orbits in the orifice region

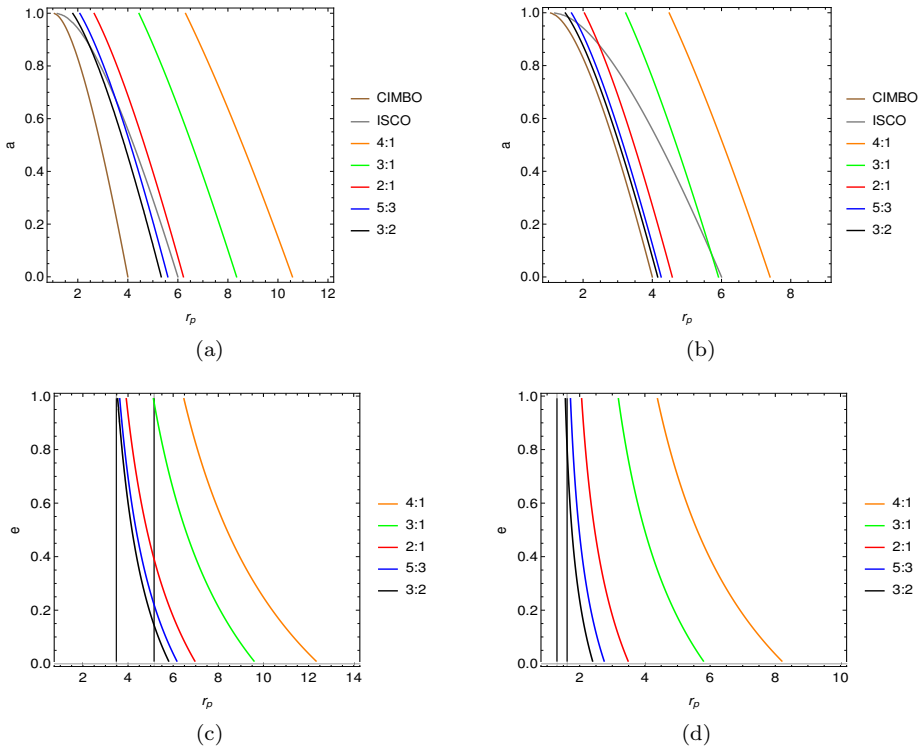

Figure 1: The frequency ratio $\nu_\phi/(\nu_\phi - \nu_r)$ contours in $(a,\ r_p)$ plane for different eccentricities, (a) $e = 0.3$, (b) $e = 0.9$, and in $(e,\ r_p)$ plane for different spin values, (c) $a = 0.25$, (d) $a = 0.98$.

stronger. We further examine the contours of the $P(\mathcal{R})$ in the $(\mathcal{R}, e)$ plane for these three regions, shown in Figs. 2(a)-2(c). It is seen that for the orifice region, fig. 2(a), $P(\mathcal{R})$ peaks near ($e = 0.5$; R =1.5-1.7), whereas for the other two cases, shown in Figs. 2(b), 2(c), $P(\mathcal{R})$ peaks for ($e < 0.4$; $\mathcal{R}$ =2-3). Under the assumption that accretion disk has its inner edge at ISCO, the orifice is likely to be vacuous. There is a possibility, supported by the above argument, that before falling into the black hole the instabilities in the accretion disk make the blobs to oscillate in an eccentric orbit with its periastron in the orifice giving rise to HFQPOs with the most probable frequency ratio 3:2.

3 Parameter estimation from RP model for QPOs

We take a more generalized approach to the RP model and consider that the orbit of the self-emitting blob can have any eccentricity and find the (e, r_p, a) of the orbit in the equatorial plane, by using the fundamental frequency formulae [15]. We apply this method to various BHXRB with three or two simultaneous QPOs, where we assume the mass measured from optical and infrared observations and spin of the black hole obtained by the fitting to the Fe Kα line or to the continuum spectrum; see Table 1.

All the solutions of (e, r_p, a) for the sources, given in Table 1, are tabulated in Table 2. For the case of GROJ 1655-40, the exact solution for e, r_p and a was not found for the centroid QPO frequencies by simultaneously solving the equations $\nu_\phi = \nu_{10}$, $\nu_\phi - \nu_r = \nu_{20}$ and $\nu_\phi - \nu_\theta$ or $\nu_{LT} = \nu_{30}$. Hence, the solution was taken at the peak value of normalized probability density for the case of $\nu_{30} = \nu_\phi - \nu_\theta$ (the peak probability for $\nu_{30} = \nu_{LT}$ is a factor of a million smaller), which is in close proximity to the centroid frequencies and well within the given 1σ errors. For the case of M82X-1, two exact solutions were found with $\nu_{30} = 210$mHz, one by using $\nu_\phi - \nu_\theta = \nu_{30}$ and the other by solving $\nu_{LT} = \nu_{30}$, where ν_{LT} is the Lense-Thirring precession frequency given by [7]

$$\nu_{LT} = \frac{2a\mu^3c^3\left(1-e^2\right)^{3/2}}{2\pi GM} = \frac{a\mu^3c^3\left(1-e^2\right)^{3/2}}{\pi GM}. \tag{1}$$

The solution found using ν_{LT} for the case of M82X-1 has a slightly higher value of a as compared to the solution found using ν_θ, this is because the Lense-Thirring frequency is directly proportional to a. The probability density peaks naturally at non-zero eccentricities for most of the sources and hence the best fit solution shows that the orbits are eccentric, which validates the importance of our analytic results for eccentric orbits.

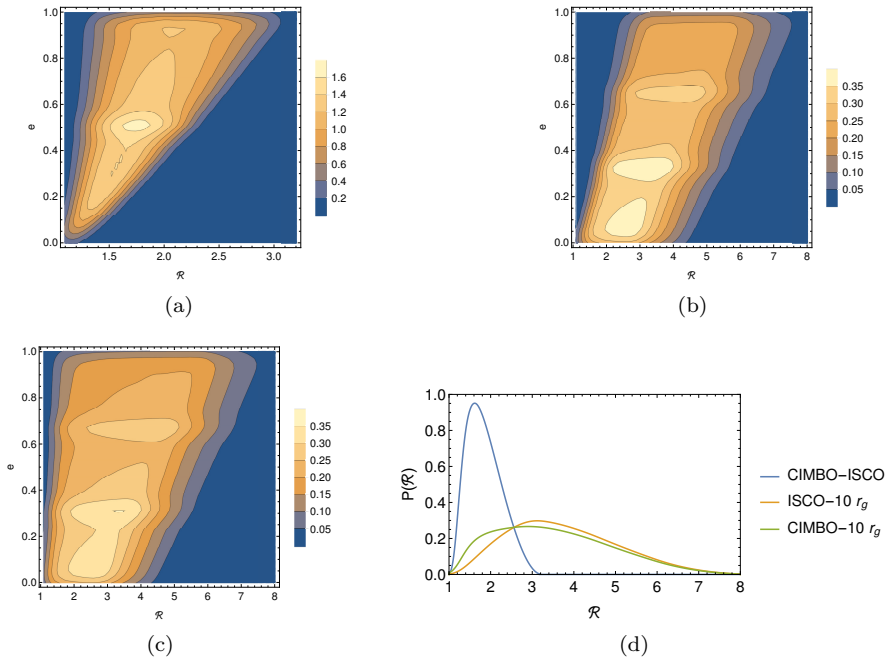

Figure 2: The figures show the contours of $P(\mathcal{R})$ in the $(\mathcal{R}, e)$ plane for the all allowed combinations of (e, r_p, a) shown for (a) in the orifice, where the $P(\mathcal{R})$ is peaking for $\mathcal{R}$ between 1.5-1.7 and e near 0.5, (b) in the disk, where $P(\mathcal{R})$ peaks for ($\mathcal{R}$ =2-3; e =0-0.4), and (c) for the entire region between CIMBO and 10 r_g, where $P(\mathcal{R})$ peaks for ($\mathcal{R}$ =2-3; e <0.4). Figure (d) shows $P(\mathcal{R})$ as a function of $\mathcal{R}$ for all these three different regions as indicated by the legends, where only for the orifice, $P(\mathcal{R})$ peaks near $\mathcal{R}$ =1.5.

S.No	Source	ν_1 Hz	ν_2 Hz	ν_3 Hz	$M/M_\odot$	a	References
1.	GROJ1655-40	441±2*	298±4*	17.3±0.1*	5.4±0.3†	-	[11]*, [21]*, [16]*, [1]†
2.	M82X-1	5.07±0.06*	3.32±0.06*	37 mHz* 120 mHz* 210 mHz*	428±105*	-	[14]*
3.	XTE J1550-564	268±3*	188±3*	-	9.1±0.61†	0.55±0.22‡; $0.34^{+0.37}_{-0.45}$ *	[17]*, [9]*, [12]*, [13]†, [20]‡, [10]*
4.	4U1630-47	179.3±5.7*	38.06±7.3*	- -	10±0.1†	$0.985^{+0.005}_{-0.014}$ ‡	[6]*, [18]†, [10]‡, [5]‡
5.	GRS1915+105	69.2±0.15*	41.5±0.4*	- -	10.1±0.6†	0.98±0.01‡	[22]*, [2]*, [3]*, [19]†, [8]‡

Table 1: The table presents the existing cases of BHXRB with simultaneous twin high-frequency QPOs, having a characteristic frequency ratio. The first two rows present the cases with three simultaneous QPOs (2 high frequency and one low frequency) and the remaining rows, the cases with two simultaneous high-frequency QPOs. The references with corresponding QPOs detection are indicated by $\star$, † marks the references with mass detection and ‡ or $*$ represents the references of spin detection.

The Fig. 3(a) shows the solutions for the frequency ratio 3:2 in the (r_p, a) plane that lie in the region bounded by the contours corresponding to $e = 0$ and $e = 0.99$. This indicates that the simultaneous HFQPOs with 3:2 ratio are likely to be generated by the eccentric orbits in this bounded region. Similarly, Fig. 3(b) shows that all the solutions in the (r_p, e) plane lie inside the region between the bounding contours $a = 10^{-5}$ and $a = 0.99$. This also implies that the simultaneous HFQPOs with 3:2 frequency ratio are likely to be generated by eccentric orbits and should be originating from the orifice. For the cases with 3:2 QPO frequency ratio, the Fig. 3(c) shows solutions in the (e, a) plane bounded by the theoretical curves for 3:2 with different values of r_p, which again confirms that the eccentric solutions of simultaneous HFQPOs with 3:2 ratio are generated in the region roughly between $r_p = 2$ to $r_p = 6$. Hence, as the results above imply that the orifice is an important region for 3:2 commensurability through eccentric orbits.

S.No	Source	e_0	σ_e	a_0 (given* /calculated†)	σ_a	r_{p0} (r_g)	σ_{r_p} (r_g)
1.	GROJ1655-40	0.072	0.0465	0.283†	0.0025	5.262	0.0922
2.	M82X-1	0.291$^\triangleright$ 0.355$^\wedge$	0.0536$^\triangleright$ 0.0839$^\wedge$	0.295$^{\triangle,\dagger}$ 0.332$^{\wedge,\dagger}$	0.0056$^\triangle$ 0.0176$^\wedge$	4.559$^\triangle$ 4.282$^\wedge$	0.1071$^\triangle$ 0.3091$^\wedge$
3.	XTE J1550-564	0.268	0.0092	0.34*	+0.37, -0.45	4.352	0.0187
4.	4U1630-47	0.734‡ 0.879$^\diamond$	0.0536‡ 0.0236$^\diamond$	0.985*	+0.005 -0.014	2.248‡ 1.396$^\diamond$	0.2982‡ 0.0598$^\diamond$
5.	GRS1915+105	0.919	0.0017	0.98*	$\pm$0.01	1.744	0.0222

Table 2: The table shows the estimated value of eccentricity, periastron distance of the orbit generating simultaneous QPOs in BHXRB and spin of the black hole and their corresponding 1σ errors using the RP model, where * represents the cases where a is obtained from previously measured fits to the Fe Kα line or to the continuum spectrum (see Table 1) and † represents the cases where a is evaluated by our method. For the case of 4U1630-47 the parameters were calculated by two methods; ‡ represents the case where the parameters were calculated by considering the two QPOs equal to ν_ϕ and $(\nu_\phi - \nu_\theta)$ and $^\diamond$ represents the case where the parameters were calculated by considering the two QPO frequencies equal to $(\nu_\phi - \nu_r)$ and ν_{LT} (Eq. (1)). For M82 X-1, $^\triangle$ represents the case where the low-frequency Type-C QPO was equated to ν_{nod} and $^\wedge$ represents the case where it was taken to be ν_{LT}. We used a Gaussian filter for GRS1915+105 and 4U1630-47 to reduce the noise in the probability density data.

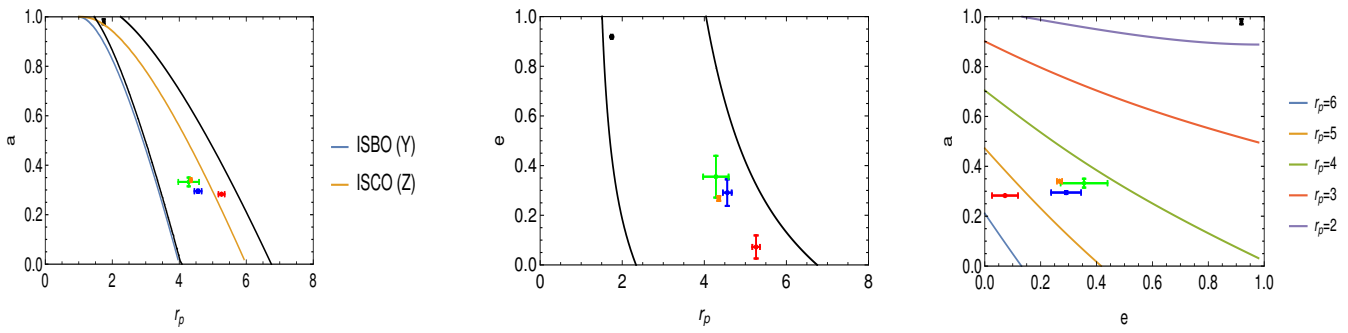

(a) (b) (c)

Figure 3: The figure shows the solutions for BHXRB (also see Table (2) in the parameter space. The points with red, blue, green, orange, and black colors represent the solution for GRO J1655-40, M82 X-1 $(\nu_\phi - \nu_\theta)$, M82 X-1 (ν_{LT}), XTE J1550-564, and GRS 1915+105 respectively. Panel (a) shows the solutions for the objects with 3:2 HFQPO frequency ratios in $(r_p,\, a)$ plane, where the black contours represent curves with frequency ratio, $\nu_\phi / (\nu_\phi - \nu_r) = 3/2$, with the inner one corresponding to $e = 0.99$, while the outer one corresponds to $e = 0$. Panel (b) only for the objects with 3:2 HFQPO frequency ratios in $(r_p,\, e)$ plane. The inner black contour represents a curve with frequency ratio, $\nu_\phi / (\nu_\phi - \nu_r) = 3/2$, corresponding to $a = 0.99$, whereas the outer black contour with the same frequency ratio corresponds to $a = 10^{-5}$. Panel (c) shows the solutions in the $(e,\, a)$ plane and the contours represent the 3:2 frequency ratio, $\nu_\phi / (\nu_\phi - \nu_r) = 3/2$, curves for different values of r_p indicated in legend.

4 Summary and discussion

We study the possible region of generation of 3:2 commensurability of HFQPOs around Kerr black hole in BHXRB. Assuming the RP model, we study the case of equatorial orbits and find that the orifice is an important region for the generation of these frequencies. We take up the specific cases of BHXRB where three or two simultaneous QPOs are observed and find the parameters $(e,\, r_p,\, a)$, Table 2, by applying the RP model for equatorial eccentric orbits using the fundamental frequency formulae. We find that the eccentric orbit solutions are possible and the orbits in the orifice region are most probable to generate 3:2 commensurability. This implies that, assuming the accretion disk ends at ISCO, the instabilities falling into the black hole from ISCO might follow eccentric trajectories in the orifice region producing HFQPOs in 3:2 resonance.

References

[1] M. E. Beer and P. Podsiadlowski. The quiescent light curve and the evolutionary state of GRO J1655-40. *MNRAS*, 331:351–360, March 2002.

[2] T. M. Belloni and D. Altamirano. Discovery of a 34 Hz quasi-periodic oscillation in the X-ray emission of GRS 1915+105. *MNRAS*, 432:19–22, June 2013.

[3] T. M. Belloni and D. Altamirano. High-frequency quasi-periodic oscillations from GRS 1915+105. *MNRAS*, 432:10–18, June 2013.

[4] T. M. Belloni and L. Stella. Fast Variability from Black-Hole Binaries. *Space Science Reviews*, 183:43–60, September 2014.

[5] A. L. King, D. J. Walton, J. M. Miller, D. Barret, S. E. Boggs, F. E. Christensen, W. W. Craig, A. C. Fabian, F. Fürst, C. J. Hailey, F. A. Harrison, R. Krivonos, K. Mori, L. Natalucci, D. Stern, J. A. Tomsick, and W. W. Zhang. The Disk Wind in the Rapidly Spinning Stellar-mass Black Hole 4U 1630-472 Observed with NuSTAR. *Astrophys. J.*, 784:L2, March 2014.

[6] M. Klein-Wolt, J. Homan, and M. van der Klis. High frequency features in the 1998 outburst of 4U 1630-47. *Nuclear Physics B Proceedings Supplements*, 132:381–386, June 2004.

[7] B. Mashhoon, F. W. Hehl, and D. S. Theiss. On the gravitational effects of rotating masses - The Thirring-Lense Papers. *General Relativity and Gravitation*, 16:711–750, August 1984.

[8] J. M. Miller, M. L. Parker, F. Fuerst, M. Bachetti, F. A. Harrison, D. Barret, S. E. Boggs, D. Chakrabarty, F. E. Christensen, W. W. Craig, A. C. Fabian, B. W. Grefenstette, C. J. Hailey, A. L. King, D. K. Stern, J. A. Tomsick, D. J. Walton, and W. W. Zhang. NuSTAR Spectroscopy of GRS 1915+105: Disk Reflection, Spin, and Connections to Jets. *Astrophys. J.*, 775:L45, October 2013.

[9] J. M. Miller, R. Wijnands, J. Homan, T. Belloni, D. Pooley, S. Corbel, C. Kouveliotou, M. van der Klis, and W. H. G. Lewin. High-Frequency Quasi-Periodic Oscillations in the 2000 Outburst of the Galactic Microquasar XTE J1550-564. *Astrophys. J.*, 563:928–933, December 2001.

[10] M. C. Miller and J. M. Miller. The masses and spins of neutron stars and stellar-mass black holes. *PhysRep*, 548:1–34, January 2015.

[11] S. E. Motta, T. M. Belloni, L. Stella, T. Muñoz-Darias, and R. Fender. Precise mass and spin measurements for a stellar-mass black hole through X-ray timing: the case of GRO J1655-40. *MNRAS*, 437:2554–2565, January 2014.

[12] S. E. Motta, T. Muñoz-Darias, A. Sanna, R. Fender, T. Belloni, and L. Stella. Black hole spin measurements through the relativistic precession model: XTE J1550-564. *MNRAS*, 439:L65–L69, March 2014.

[13] J. A. Orosz, J. F. Steiner, J. E. McClintock, M. A. P. Torres, R. A. Remillard, C. D. Bailyn, and J. M. Miller. An Improved Dynamical Model for the Microquasar XTE J1550-564. *Astrophys. J.*, 730:75, April 2011.

[14] D. R. Pasham, T. E. Strohmayer, and R. F. Mushotzky. A 400-solar-mass black hole in the galaxy M82. *Nature*, 513:74–76, September 2014.

[15] P. Rana and A. Mangalam. Dynamics of bound orbits in Kerr geometry and application to QPOs in BHXRB, Submitted. *Submitted to Phys. Rev. D.*, 2017.

[16] R. A. Remillard, E. H. Morgan, J. E. McClintock, C. D. Bailyn, and J. A. Orosz. RXTE Observations of 0.1-300 HZ Quasi-periodic Oscillationsin the Microquasar GRO J1655-40. *Astrophys. J.*, 522:397–412, September 1999.

[17] R. A. Remillard, M. P. Muno, J. E. McClintock, and J. A. Orosz. Evidence for Harmonic Relationships in the High-Frequency Quasi-periodic Oscillations of XTE J1550-564 and GRO J1655-40. *Astrophys. J.*, 580:1030–1042, December 2002.

[18] E. Seifina, L. Titarchuk, and N. Shaposhnikov. Black Hole Mass Determination in the X-Ray Binary 4U 1630-47: Scaling of Spectral and Variability Characteristics. *Astrophys. J.*, 789:57, July 2014.

[19] D. Steeghs, J. E. McClintock, S. G. Parsons, M. J. Reid, S. Littlefair, and V. S. Dhillon. The Not-so-massive Black Hole in the Microquasar GRS1915+105. *Astrophys. J.*, 768:185, May 2013.

[20] J. F. Steiner, R. C. Reis, J. E. McClintock, R. Narayan, R. A. Remillard, J. A. Orosz, L. Gou, A. C. Fabian, and M. A. P. Torres. The spin of the black hole microquasar XTE J1550-564 via the continuum-fitting and Fe-line methods. *MNRAS*, 416:941–958, September 2011.

[21] T. E. Strohmayer. Discovery of a 450 HZ Quasi-periodic Oscillation from the Microquasar GRO J1655-40 with the Rossi X-Ray Timing Explorer. *Astrophys. J.*, 552:L49–L53, May 2001.

[22] T. E. Strohmayer. Discovery of a Second High-Frequency Quasi-periodic Oscillation from the Microquasar GRS 1915+105. *Astrophys. J.*, 554:L169–L172, June 2001.